



Assessing building thermal resilience in response to heatwaves through integrating a social vulnerability lens

Suman Paneru ^a, Xinyue Xu ^a, Julian Wang ^a, Guangqing Chi ^b, Yuqing Hu ^{a,*}

^a Department of Architectural Engineering, Penn State University, University Park, PA, 16802, USA

^b Department of Agricultural Economics, Sociology, and Education, Penn State University, University Park, PA, 16802, USA



ARTICLE INFO

Keywords:

Gaussian naïve bayes model
Social vulnerability
Thermal resilience
Thermal physics
Equity

ABSTRACT

Major cities worldwide are increasingly experiencing intense heatwaves, which disproportionately affect vulnerable populations. This suggests the urgent need for focused attention and mitigation strategies to protect those most at risk from the impacts of heatwaves. The presence of vulnerable groups in buildings with varying thermal conditions can result in different outcomes during extreme heat events, making it crucial to evaluate the thermal resilience of buildings in conjunction with social vulnerability. This research advances the understanding of thermal vulnerability by integrating building thermal characteristics with social vulnerability. While previous studies have predominantly focused on socio-ethnic and economic dimensions of vulnerability, this study specifically investigates the relationship between social vulnerability and thermal resilience, with a focus on building thermal parameters. Datasets from Zillow and ResStock are used to capture the thermal properties of buildings, while social vulnerability data is obtained from the Center for Disease Control and Prevention. A Gaussian Naïve Bayes (GNB) model is applied to enhance building envelope attributes from Zillow, leveraging detailed information from ResStock data. Additionally, a Kolmogorov-Smirnov (KS) test is conducted to analyze diverse thermal attributes, such as age of buildings, room size, number of stories, building area, envelope characteristics, systems, infiltration, across differing levels of social vulnerability (high and low). Specifically, Philadelphia is selected as the analysis focus. The analysis reveals significant associations between thermal resilience and social vulnerability. Groups with higher social vulnerability are more likely to be exposed to elevated levels of thermal vulnerability compared to less vulnerable groups. This highlights the necessity for tailored interventions aimed at promoting the development of more resilient and equitable buildings, capable of reducing the impacts of heatwaves on vulnerable communities.

1. Introduction

Climate change is significantly amplifying global exposure to extreme heat. Between 2000–2004 and 2017–2021, heat-related fatalities among individuals over the age of 65 increased by approximately 85 % [1,2]. According to World Health Organization, about 125 million people experienced heatwaves globally between 2000 and 2016 [3], with the 2003 European heatwave alone resulting in over 70,000 excess deaths [4]. The frequency of annual heatwaves has steadily risen, from an average of two per year

* Corresponding author.

E-mail address: yh5204@psu.edu (Y. Hu).

globally in the 1960s to six in the 2010s and 2020s; with each heatwave now lasting an average of four days, approximately one day longer than those in the 1960s [5]. Vulnerable groups, including the elderly, individual with preexisting health conditions, socio-economically disadvantaged populations, and historically underrepresented minorities, are disproportionately affected by the adverse effects of heatwaves [6–8]. Current global warming trends project further rise in the frequency, intensity, and duration of heatwaves, placing an even larger proportion of the population at risk [9], thus underscoring the critical importance of enhancing thermal resilience. The health impacts of these heat events are severe, with heightened health risks directly proportional to the intensity of heatwave [10]. Furthermore, historical data reveal a consistent pattern of increased morbidity and mortality rates during the heatwaves, particularly among the most vulnerable populations [11], exposing the inadequacy of existing buildings in protecting communities from heat-related illness and exacerbating the crisis.

Social Vulnerability refers to the susceptibility of individuals or communities to adverse effects, whether from natural hazards, human-caused disasters, or disease outbreaks, shaped by a complex interplay of physical, social, economic, and environmental factors [12–14]. Recent studies conducted in England and Brazil have highlighted the disproportionate effects of extreme heatwaves on vulnerable groups, particularly the elderly and socioeconomically disadvantaged [7,8]. Households characterized by lower socioeconomic status, minority communities, or those with younger residents may experience the impact of heatwaves in unique and more severe ways [15]. Therefore, resource allocations should consider social vulnerabilities to ensure service disruptions during extreme heatwaves do not disproportionately burden already vulnerable populations [16]. These vulnerabilities are often deeply embedded within socioeconomic structures, which can outweigh geographic or physical exposure to climate-related hazards such as heatwaves [17]. For example, two neighboring communities may exhibit vastly different vulnerability profiles depending on their socio-economic dynamics, even when exposed to the same extreme heatwaves or other weather events. Research suggests that regions with high social vulnerability frequently demonstrate lower resilience, as seen in areas of the U.S. West where vulnerability is pronounced, and the Southeast where resilience is reduced [18]. This underscores the critical need to address the intersection of social vulnerability and resilience, as socially vulnerable communities are often less equipped to withstand and recover from the impacts of extreme heat, further exacerbating inequalities in health and well-being.

Resilience is the capacity of a system, community, or individual to anticipate, adapt to, and recover from disruptions or changing conditions while maintaining essential functions and undergoing positive transformation in the face of long-term stresses, challenges, and uncertainties [19–24]. The infrastructure supporting resilience must be robust and adaptable, fostering economic growth and innovation [25]. As essential services are disrupted, the ability of communities to cope during crises tend to decrease in a nonlinear fashion, highlighting the critical need for resilient systems [26]. With the intense heatwaves, enhancing thermal resilience in buildings and community infrastructures has become increasingly urgent. This is essential not only to protect populations but also to prevent some cities from approaching uninhabitable conditions [27,28]. Thermally resilient buildings play a key role in mitigating the strain on essential urban systems throughout all phases—before, during, and after heatwaves. Furthermore, buildings significantly influence vulnerability to extreme heat events [29]. Improved building resilience can alleviate some of the adverse impacts of heatwaves, safeguarding both human health and broader urban systems [30]. Central to the challenge of thermal resilience is the concept of thermal equity, which addresses the inequitable distribution of heat-related risks across different populations within urban areas [31]. Thermal equity policies aim to mitigate the unequal exposure to extreme heat, particularly in neighborhoods where socio-demographic factors such as race and income are linked to heightened vulnerability [32]. By addressing both resilience and equity, cities can work to reduce disparities in heat exposure and protect the most affected communities from the growing threats posed by climate change.

The importance of building features in enhancing thermal resilience has been well acknowledged in previous studies. In Phoenix, AZ, for instance, the role of building design has been linked to varied perceptions of heat levels, ranging from minor inconvenience to catastrophic threats. This highlights the potential influence of building design on residents heat related experiences [33]. However, while the Nature's cooling systems project identified adaptation challenges at the neighborhood level in Phoenix, it did not examine the specific building attributes that might mitigate or exacerbate these challenges [34]. Similarly, in Accra and Tamale, Ghana, where poor infrastructure exacerbated health vulnerabilities from urban heat, the role of specific building feature was not addressed [35]. The thermally resilient communities collaborative framework, tested in Tempe and Buffalo, emphasized the need for localized thermal management solutions [36]. Building with passive features, such as adequate insulation have shown to enhance thermal performance while improving their ability to manage heat stress [37]. In the UK, monitoring energy-efficient homes during the 2015 heatwave highlighted the significance of building features and ventilation's role in determining indoor thermal conditions [38]. A study in Australia also emphasized the value of heat-resistant buildings for boosting resilience and health, particularly those that prioritize passive design features over active measures such as air conditioning [39]. Micro-level studies further reinforce the importance of specific building features in enhancing resilience [40]. In Spain, a large proportion of residential buildings were found to lack adequate thermal protection, indicating need for updated building standards and codes to address future heatwaves challenges [41]. Research in passive building design in Argentina pointed to the necessity of updated overheating metrics that account for factors such as solar radiation [42]. In low-income housing in Argentina, a disconnect between building design and climate conditions weakened thermal resilience [43]. "Double density" housing in Montreal showcased the benefits of energy-efficient homes in fostering resilience [44], while a study in Poland demonstrated the potential of raw-earth technologies to provide sustainable thermal resilience [45]. Conversely, heritage buildings in Seville struggled to maintain thermal comfort using only passive strategies, underscoring the need for enhanced building system to ensure resilience [46]. These findings collectively emphasize the critical role of building attributes in shaping thermal resilience and highlight the need for targeted solutions that address both passive and active building strategies across diverse geographic contexts.

In the context of extreme heatwaves, socially vulnerable communities require targeted policies to ensure their protection and resilience [33]. Proactive measures that strengthen energy systems and promote the adaptation of sustainable technologies are critical

for improving resilience and mitigating the impacts of extreme events such as heatwaves [47]. Comprehensive assessments can aid policymakers in establishing equitable energy and thermal resilience guidelines across diverse communities [48,49]. Numerous studies have employed index based approaches such as the social vulnerability and the community resilience index [18,50]. However, there exists a significant gap in integrating general building information (building area and type) with thermal features (insulation and infiltration). This integration is essential for accurately assessing thermal vulnerability across different levels of social vulnerability. Therefore, addressing these gaps is crucial for developing comprehensive strategies that incorporate both building-specific characteristics and social factors, thereby enhancing resilience against escalating threat of heatwaves.

The incorporation of thermal features into vulnerability indices marks a significant advancement in understanding and addressing the resilience. While existing indices, such as the social vulnerability and the community resilience index, provide valuable insights into societal vulnerabilities, they often fall short in comprehensively accounting for the thermal characteristics of buildings and their impact on vulnerability. This study aims to bridge this gap by integrating building features with social vulnerability index to deepen our understanding of thermal vulnerability. By examining aspects of building characteristics such as the building envelope, age, insulation, and air infiltration, this research seeks to explore thermal resilience across communities with differing levels of social vulnerability. A detailed analysis is conducted to investigate how building thermal characteristics interact with their thermal vulnerability, which helps future studies on heatwaves by enriching social vulnerability indices. Ultimately, the goal is to elucidate the interplay between social and thermal vulnerabilities, thereby guiding the development of more equitable and resilient building policies.

2. Method

This study employs a methodological framework depicted in [Fig. 1](#), comprising several key stages. Initially, data is collected from various platforms, including Zillow [51], ResStock [52], and the CDC [12]. Zillow provides refined geolocation data at the individual building level, along with information on the building's year, area, number of stories, number of rooms, exterior finish, and basic building systems. ResStock offers detailed information on building prototype to specific cities, encompassing a comprehensive inventory of building stocks. This includes vintage information, area, insulation characteristics, window types, infiltration rates, heating systems. The integration of Zillow and ResStock datasets are particularly advantageous for acquiring insulation data. Naïve Bayes model (GNB) was employed for obtaining insulation data. After the enrichment of Zillow data, we aggregated household level data to match vulnerability level defined based on the CDC data. The CDC contributes valuable indices related to socioeconomic status, household features, racial and ethnic minority status, and housing and transportation metrics at a scale of census level. While the CDC's housing type and transportation index includes data on multi-unit structures, mobile homes, and homes without vehicles, it lacks specific thermal properties such as building age, number of stories, area, envelope characteristics, and building systems. Therefore, integrating data from Zillow and ResStock enhances our understanding of building features, allowing for a more thorough assessment of thermal vulnerability across vulnerable groups.

2.1. Data collection

In this research, multiple data sources were utilized, as summarized in [Table 1](#). Building features were collected from Zillow and Department of Energy ResStock database, while social vulnerability data was sourced from the Centers for Disease Control and Prevention (CDC).

The Social Vulnerability Index (SVI) from the CDC provides thematic insights capturing key factors socioeconomic status,

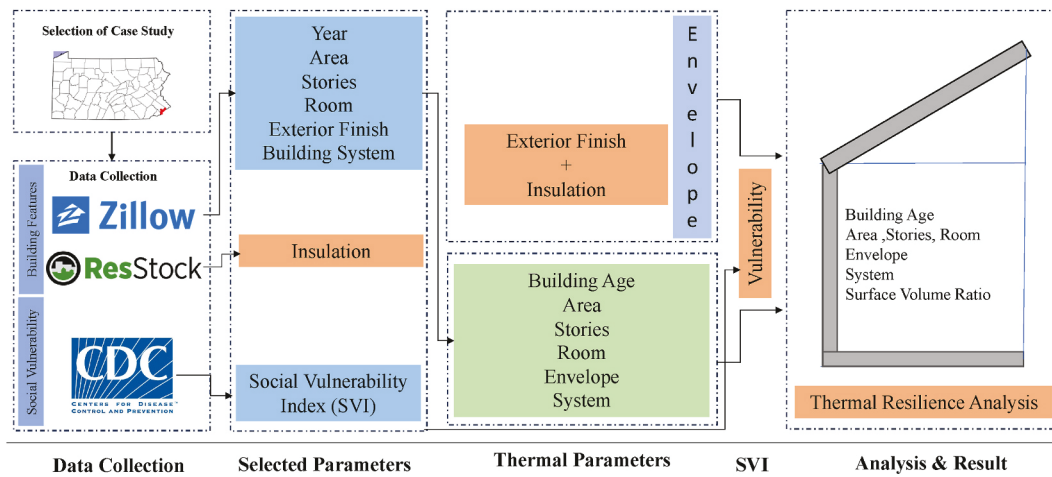


[Fig. 1.](#) Methodological framework employed in the study.

Table 1

Data sources and selected parameters utilized in the study.

Data Source	Parameters	References
Zillow	Building Features such as year, area, stories, room	[51]
Centers for Disease Control and Prevention (CDC)	Social Vulnerability Index	[12]
DoE ResStock	Building Stock Characterization	[52]

household composition, racial and ethnic minority status, and housing and transportation, along with one overall vulnerability index (RPL_Themes). In this study, the SVI overall theme index as used to classify census tracts into four vulnerability clusters-low, moderate, medium high, and high. For instance, a high-vulnerability cluster comprises percentile rankings ranging from 0.75 to 1.0, and a low-vulnerable groups from <0.250. The classification for the overall vulnerability index is shown in [Table 2](#).

The CDC obtained Social Vulnerability Index (SVI) data include RPL_Themes information at the census tract level. Using these percentile ranks, building features re-clustered according to the SVI vulnerability clusters. For simplification, all buildings within each census tract were assumed to share the same vulnerability level, classifying them into four distinct groups: low, moderate, medium high, and high vulnerability. After linking the building features with social vulnerability data, comparative analysis was performed to assess the significance of thermal features, such as building envelope, between low and high vulnerability groups. This process provided insights into the disparities in building characteristics across different levels of social vulnerability, particularly in relation to thermal resilience.

2.2. Selection of thermal resilience-related building characteristics

In the evaluation of building characteristics, the primary focus was to identify key features that significantly influence the thermal behavior of buildings, particularly in terms of resilience to heat stress. These features were chosen based on their direct impact on how buildings respond to external thermal loads, and their relevance to thermal vulnerability among different social vulnerability groups. The selected parameters are summarized in [Table 3](#). By analyzing these characteristics collectively, this study aims to assess the extent of thermal vulnerabilities between high and low vulnerable groups, providing insights into building performance under heatwaves.

2.3. Parameter enrichment

The ResStock provides detailed building prototype characteristics tailored to specific cities, that includes characteristics such as building year, area, and insulation wall types, whereas the Zillow dataset lacks this detailed information on insulation wall types. To bridge this gap, a Gaussian Naïve Bayes (GNB) classifier is developed to establish a probabilistic relationship between known building characteristics and insulation wall types based on ResStock's dataset. Known as a computationally efficient approach, the GNB yields distributions of possible wall types for each building rather than a single wall type and quantitatively indicates model confidence on predictions, which is crucial for decision-making in thermal vulnerability assessment. The GNB is trained using 80 % of the ResStock data and tested using the remaining 20 % ResStock data. Moreover, the grid search is systematically included to find the optimal combination of hyperparameters that maximize the GNB's performance. Model performance is assessed through accuracy, precision, and F1-score, as summarized in [Table 4](#). The GNB is further applied to the Zillow dataset to infer possible distributions of insulation wall types for individual buildings. In Section 3.1, uncertainty analysis is introduced to discuss predictive uncertainty associated with GNB on Zillow data. [Fig. 2](#) demonstrates the overall workflow of GNB in enriching missing features in Zillow data by leveraging more detailed ResStock data. Two input features are selected to infer the insulation wall types from the trained GNB, respectively building year and building area. Building year is selected as one critical indicator of insulation wall types since construction materials and building standards evolve over time. The building year are clustered based on the ResStock classification: <1940, 1940-59, 1960-79, 1980-99, 2000-09, and 2010s [60]. Similarly, building area often serves as a proxy for building types, each with different insulation materials due to variations in energy requirements and structural considerations. This enables a robust characterization of building envelope insulation at a finer spatial resolution.

As shown in [Table 4](#), the performance of the GNB classifier is evaluated using four performance metrics: accuracy, precision, recall and the F1-score. The evaluation was conducted on both training (80 % of ResStock data) and testing (20 % of ResStock data) datasets. The GNB achieves an accuracy of 80.9 % on the training data and 80.0 % on the testing data, indicating consistent performance across both datasets. Besides, the GNB exhibits high precision with 88.1 % on the training dataset and 88.2 % on the testing set, suggesting a low occurrence of false positive predictions. The recall values are 80.9 % for the training set and 80.0 % for the testing set. Results

Table 2

Overall tract percentile SVI rankings obtained from the CDC data.

Social Vulnerability	RPL_Themes (Percentile Ranking)
Low	<0.250
Moderate	0.26-0.50
Medium High	0.51-0.75
High	0.75-1.0

Table 3
Selected building characteristics related to thermal resilience.

Parameters	Description	References
Building age	The age of a building generally determines envelope properties and the condition of the internal building system.	[53]
Area, Story numbers, and Room numbers	The building's footprint, volume, vertical extent, and internal layout influence its general thermal performance.	[54]
Building envelope	The building envelope regulates heat exchange with the external environment, affecting thermal efficiency.	[55,56]
Building system	Building systems maintain internal temperature and reduce thermal vulnerabilities	[57]
Surface-to-Volume (S/V) ratio	The ratio of building's surface area to its internal volume, a crucial factor in heat transfer.	[58,59]

Table 4
Performance metrics on the GNB classifier based on ResStock data.

Performance metric	Math formula	Training dataset	Testing dataset	Explanation
Accuracy	$\frac{TP + TN}{TP + TN + FP + FN}$	80.9 %	80.0 %	The ratio of correctly classified instances to total instances.
Precision	$\frac{TP}{TP + FP}$	88.1 %	88.2 %	The ratio of correctly predicted instances to the total predicted positive instances.
Recall	$\frac{TP}{TP + FN}$	80.9 %	80.0 %	The ratio of correctly predicted instances to the total actually positive instances.
F1-score	$\frac{2 * TP}{2 * TP + FP + FN}$	81.4 %	80.7 %	The harmonic mean of precision and recall

Note that the classified insulation walls used for evaluation have the highest probability in a range of possible outcomes, TP and TN are the true positive and negative predictions. FP and FN are false positive and false negative values. The training dataset is 80 % of ResStock data and the testing dataset is 20 % of ResStock data.

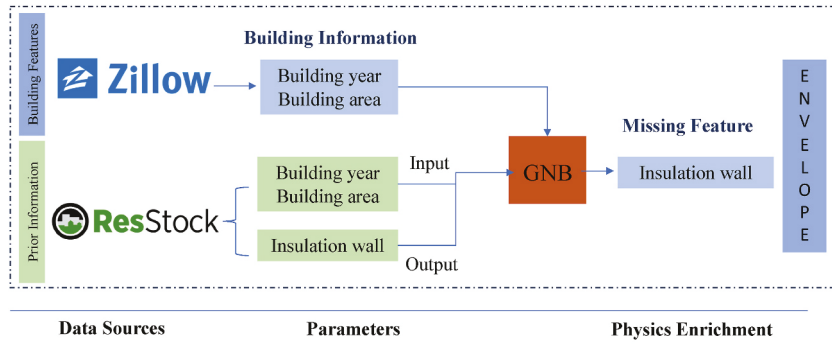


Fig. 2. Physics enrichment of the Zillow dataset.

indicate that the GNB classifier capture most of the true instance of the insulation wall types. The F1-score values for the GNB are 81.4 % and 80.7 %, respectively on the training and testing datasets. Consequently, the GNB performs well in predicting insulation wall types from building year and area, indicating its reliability and predictive capability when applying to Zillow data.

2.4. KS statistical tests

The Kolmogorov-Smirnov test (KS- test) is used to determine whether two samples differ significantly in their distribution shapes by comparing their cumulative distribution functions. It calculates the maximum vertical distance between their cumulative distribution functions. A p-value below 0.05 indicates strong evidence against the null hypothesis, suggesting that the samples likely originate from different distributions. Since the building features data from Zillow and ResStock do not follow a normal distribution, the KS test is the most suitable statistical test for this analysis. Its non-parametric nature allows it to assess distributional differences without assuming any underlying distribution, making it an ideal choice for comparing the building features across the datasets. This approach ensures a robust statistical evaluation of how closely the distributions of building features align.

3. Case study

Philadelphia was selected as the case study due to its SVI index of 1, highest within the State of Pennsylvania (PA) [12].

Additionally, data visualization for Philadelphia's vulnerability index reveals that in high-vulnerability groups, socioeconomic, racial, and housing indexes surpass the overall social vulnerability index. Conversely, in low-vulnerability groups, most indexes, except for the household characteristic index fall below the overall theme index as depicted in [Fig. 3](#). This stark contrast in housing and ethnic characteristics between the high and low-vulnerable groups suggests the need for a deeper investigation into resilience through the lens of housing characteristics and social vulnerability, particularly from a thermal perspective. This study examines 363 census tracts in Philadelphia, of which 258 tracts are classified as high-vulnerable and 40 tracts as low-vulnerable, and remaining tracts fall into the middle vulnerable based on the SVI index sourced from the CDC. In addition, data obtained from Zillow, encompasses approximately 400446 households, and ResStock which provided 2766 homes representing different vantage years, geometry, infiltration characteristics. The overall SVI (RPL_Themes) was used to categorize census tracts into high, low-medium, medium-high, and low groups. Each census tract was assigned to one of these categories based on the predominant theme of its index score. For instance, if a census tract had SVI of 0.78, all households within that tract was categorized as belonging to a high-vulnerable group.

3.1. Data analysis summary

3.1.1. Building age

[Fig. 4](#) represent the probability density of number of residential buildings constructed in Philadelphia per year between high and low-vulnerable groups. Analysis of Zillow data indicates that a significant proportion of homes associated with high-vulnerability groups were built before 1960, while a greater number of homes constructed 1980 are part of the low-vulnerability groups. While this observation doesn't directly establish a causal link between social vulnerability and building resilience, it highlights the potential risk: high-vulnerability groups may be more exposed to heatwaves due to their higher likelihood of residing in older homes, which are often higher infiltration, and less efficient. This aligns with Aksoezen et al.'s [53] study, which identified a correlation between building age and energy performance in Basel, Switzerland. In Philadelphia, the high-vulnerability group is particularly susceptible to thermal risks, as many of their homes were built before 1940, suggesting potential deficiencies in insulation and building envelope performance. The KS test, which yielded a statistic of 0.27 with a P-value less than 0.05, further confirms a significant difference in the distribution of building ages high and low vulnerable groups. This emphasizes the importance of addressing the thermal vulnerabilities of older housing stock in socially vulnerable communities.

3.1.2. Stories, room numbers, and areas

The area of building, number of stories, and number of rooms in a building offer insight into both the social status and social vulnerability of its residents. From a thermal vulnerability perspective, these characteristics significantly influence a building's thermal mass and inertia, which play key roles in its ability to buffer and moderate temperature changes caused by external weather conditions. Buildings with more stories typically exhibit improved thermal inertia due to a lower surface area to volume ratio, which helps to retain and distribute heat more effectively. Additionally, a higher number of rooms allow for precise thermal zoning, where interior wall partitions further enhance thermal regulation and resilience against outdoor temperature fluctuations. Larger building areas also provide opportunities for optimal layout and orientation, making it easier to avoid solar heat gains and optimize ventilation, ultimately improving the thermal resilience of buildings. As depicted in [Fig. 5 \(a\)](#), the KS result of 0.356 with a P-value less than 0.05 suggests a statistically significant difference in the number of rooms between high and low-vulnerable groups. Additionally, the analysis suggests that homes in low-vulnerable groups are generally larger compared to the high-vulnerable groups.

The data reveals a distinct disparity in building characteristics between low-vulnerable and high-vulnerable groups, particularly in the number of rooms. As depicted in [Fig. 5\(b\)](#), low vulnerable groups tend to occupy homes with more rooms compared to high-vulnerable counterparts. A KS test of 0.148 and a P value of <0.05 further corroborates this significant difference in room

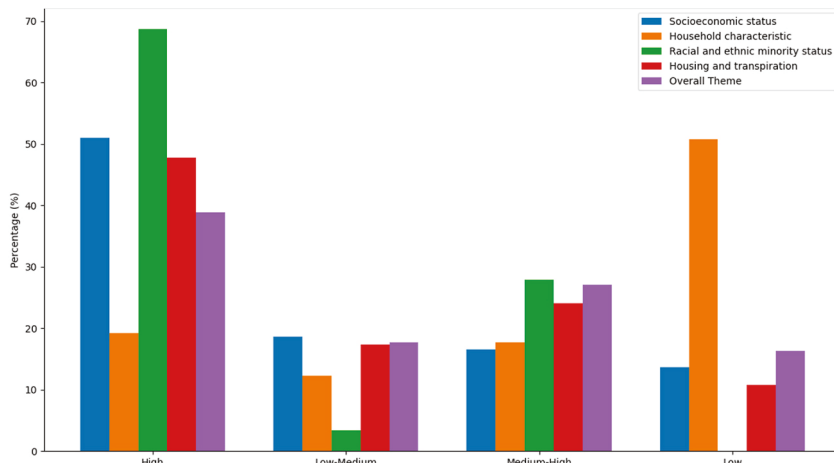


Fig. 3. Distribution of RPL_Themes for various vulnerability groups.

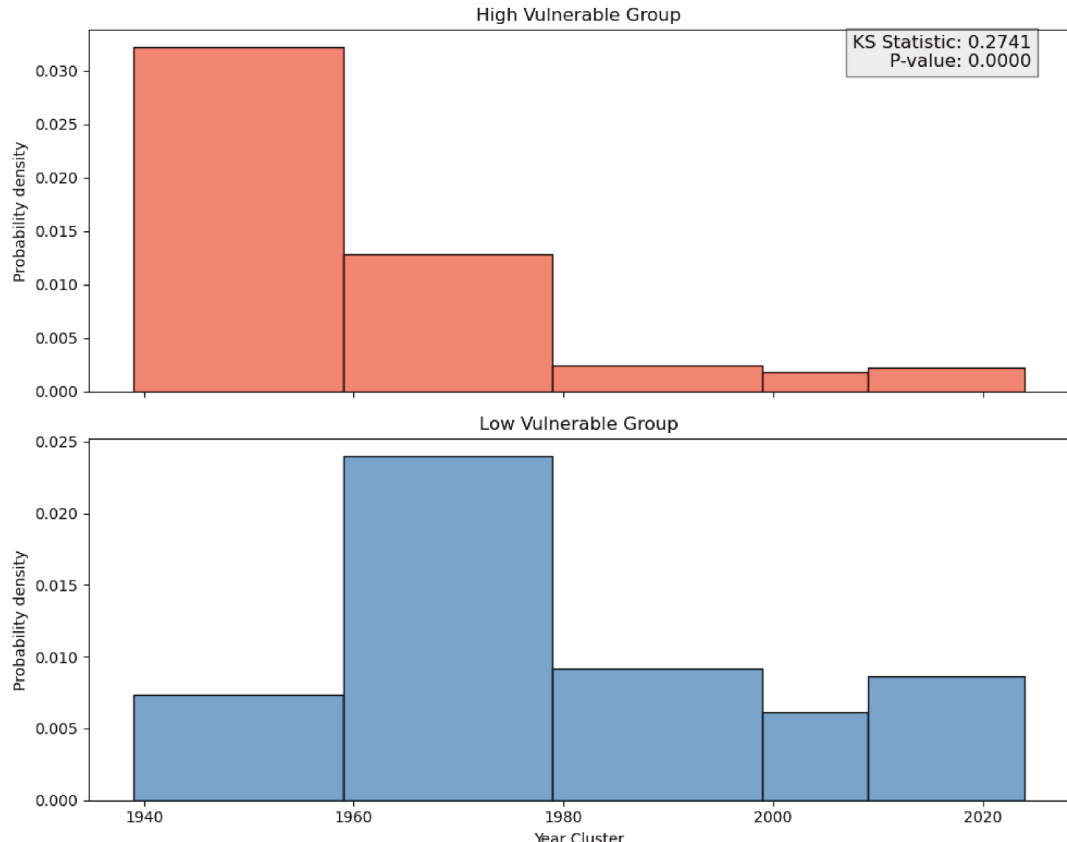
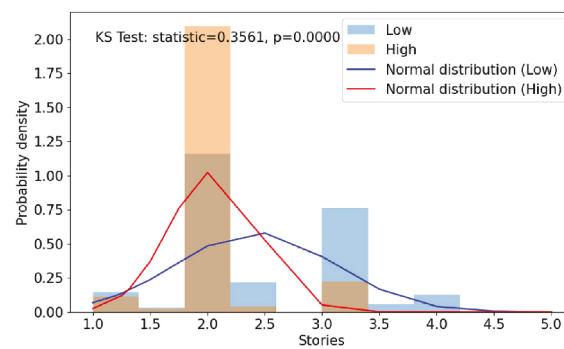


Fig. 4. Probability density of number of homes based on the building age.

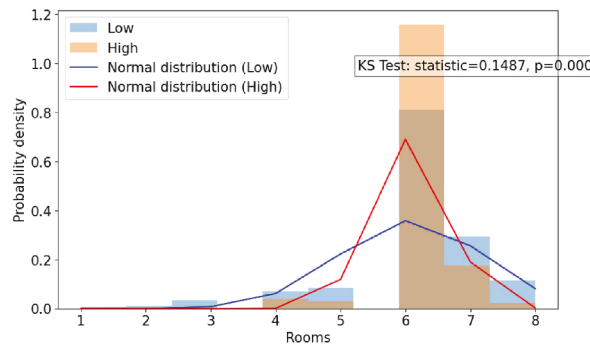


(a): probability density of stories between low and high-vulnerable

Fig. 5 (a). probability density of stories between low and high-vulnerable.

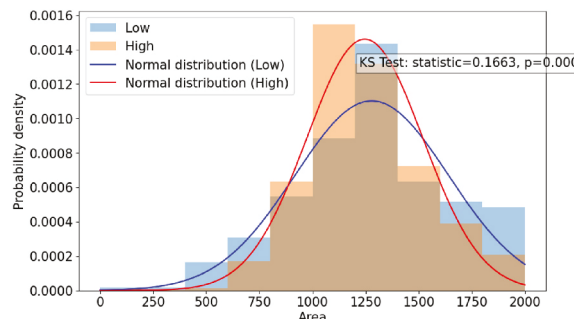
numbers, which is crucial in understanding the relationship between social and thermal vulnerabilities. In addition, home size (area), as a key thermal parameter, was further analyzed based on common thresholds in PA. With the median home size in PA is approximately 2000 sq ft, homes were categorized into three size groups: below 2000 sq ft, between 2000 and 3000 sq ft, and above 3000 sq ft. Fig. 5(c) shows that homes smaller than 1500 sq ft are more prevalent among high-vulnerable groups, which align with a KS statistic of 0.166 and a P value < 0.05 , indicating a significant difference. Conversely, Fig. 5(d) reveals that low vulnerable groups predominantly occupy homes larger than 3000 sq ft, as demonstrated by a KS test score of 0.108 and a P value < 0.05 .

In summary, the analysis highlights that low social-vulnerable groups typically reside in homes with more stories, rooms, and larger areas-factors that contribute top better thermal resilience. These building features enhance thermal mass and inertia, help mitigate the impacts of outdoor temperature fluctuations. In contrast, high-vulnerable groups, with fewer rooms and smaller home sizes are more



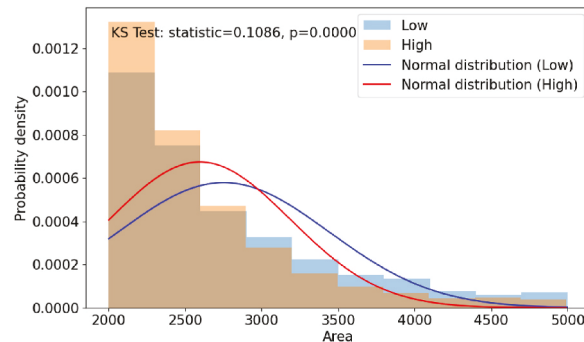
(b): probability density of rooms between low and high-vulnerable

Fig. 5 (b). probability density of rooms between low and high-vulnerable.



(c): probability density of area less than 2000 sq ft between low and high-vulnerable

Fig. 5(c). probability density of area less than 2000 sq ft between low and high-vulnerable.



(d): probability density of area larger than 3000 sq ft between low and high-vulnerable

Fig. 5(d). probability density of area larger than 3000 sq ft between low and high-vulnerable.

susceptible to thermal stress, highlighting a significant intersection between social and thermal vulnerability.

3.1.3. Building envelope

The building envelope plays as a pivotal role in maintaining thermal performance, particularly during extreme heatwaves. Critical properties such as thermal resistance (R-value) and capacitance influence how well a building can retain or resist heat. However, the Zillow dataset lacks explicit information about the R value of insulation. As shown in Fig. 6, most residential buildings in Philadelphia have brick exteriors based on Zillow dataset, but it does not include specific details about the R-value of these envelope. To bridge this

gap, a Gaussian Naïve Bayes (GNB) model was used to probabilistically estimate missing feature — specifically, the R-value for building envelopes in the Zillow dataset. The necessary R-value information was sourced from ResStock, which includes comprehensive details about the building year, area, and types of insulations.

For the GNB imputation, the building year data from Zillow was categorized into six intervals to align with the vintage years defined by ResStock. ResStock includes 13 distinct wall insulation types, providing details on the exterior envelope and insulation (e.g., "Brick, 12-in, 3 wythe, uninsulated" and "CMU, 6-in Hollow, uninsulated" were grouped as R-0). Insulation types with similar R-values were consolidated, resulting in five main categories: R-0, R-7, R-11, R-15, and R-19. The GNB model was employed to probabilistically assign an insulation type based on the building year and building area. This imputation model helps fill the gaps in the Zillow data by integrating the probabilistic distribution from ResStock.

Fig. 7(a) illustrates the distribution of building years and insulation types from the ResStock dataset, while Fig. 7(c) depicts the distribution of building areas and insulation types. In both figures, the bubble sizes represent the frequency of each combination. Smaller bubbles, such as those corresponding to buildings from 1940-59 and 1980-99 with R0 insulation, indicate less-common combinations compared to the more prevalent combination of buildings constructed before 1940 with R0 insulation. Additionally, the clustering of bubbles around R0 insulation and building areas under 2000 sq ft suggests a correlation between building year, insulation type, and area. As a result, the GNB model used these features—year and area—to enhance the enrichment of the Zillow data. After GNB enrichment, Fig. 7(b) presents the distribution of enriched wall insulation types, while Fig. 7(d) shows the distribution of building areas, both determined by their highest probability. Fig. 8 illustrates the envelope's R value for the year clusters derived from GNB imputations for both high and low-vulnerable groups. Clearly, uninsulated envelope dominates the city of Philadelphia further confirming the high social vulnerability of the region. The limited availability of information on R-15 and R-11 insulation types during the periods of 1980-99 and 2000-09 may be contributing to the increased uncertainty observed in the enriched Zillow data.

A KS-test was performed to evaluate the statistical significance of various envelope between high and low vulnerable groups. The results, presented in Table 5, reveal that uninsulated walls, indicate substantial deviations for uninsulated walls, with KS test statistic of 1.00 and a P value of <0.05 , indicates high statistical significance. For envelope with various R-values (R-7, R-11, R-15, and R-19), the KS test results exhibit a range of significance. The KS statistic for R-7 is 0.812, with a p-value <0.05 , suggesting moderate significance, while for R-11, the KS statistic is lower at 0.042. These results indicate that higher R-values tend to reduce the significance of the thermal differences. For R-11, the KS Statistic is 0.042, indicating a much weaker distinction between insulated and uninsulated versions. However, R-15 has a KS Statistic of 1.00, suggesting a high level of significance in certain cases. An uncertainty analysis has been conducted to account for the uncertainty that may have existed in the GNB model during the imputation process.

3.1.3.1. Uncertainty analysis. Here we carry out uncertainty analysis by measuring probabilistic entropy across all predicted probabilities [61], as illustrated in Eq. (1):

$$H(x) = - \sum_{i=1}^N (p_i * \ln p_i) \quad \text{Eq. (1)}$$

where H is the total entropy over the predicted probabilities for one building, p_i is the predicted probability for the i th insulation wall type, N is the total number of insulation wall types.

For a 5-class classification problem, we define threshold values of 0.78 as low entropy and 1.61 as high entropy to show a spectrum of predictive uncertainty. In a scenario with high entropy, predicted outcomes are often uniformly distributed, exhibiting large uncertainty and low confidence across all five classes. For example, each insulation type has an equal probability of $1/5$, resulting in $H_{high} = -5 * \left(\frac{1}{5} * \ln \frac{1}{5}\right) = 1.61$. In contrast, an acceptable scenario with low entropy would predict one insulation wall type with a high probability (i.e., 80 %) and impose the remaining probability (i.e., 20 %) evenly on other four types, $H_{low} = - (0.8 * \ln 0.8) - 4 * \left(\frac{0.2}{4} * \ln \frac{0.2}{4}\right) = 0.78$.

Table 6 provides the probability distributed across all insulation wall types for nine buildings, where predictions with the highest

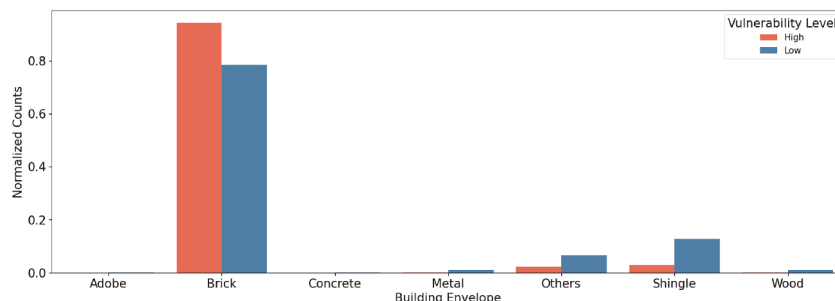
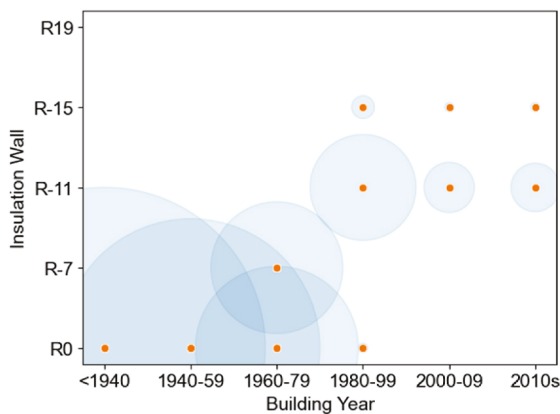
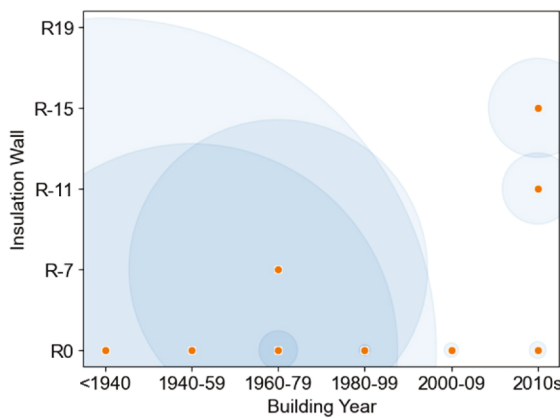


Fig. 6. Building exterior finish based on Zillow data.



(a) ResStock building year and insulation distribution

Fig. 7 (a). ResStock building year and insulation distribution.



(b) Enriched building year and insulation distribution

Fig. 7 (b). Enriched building year and insulation distribution.

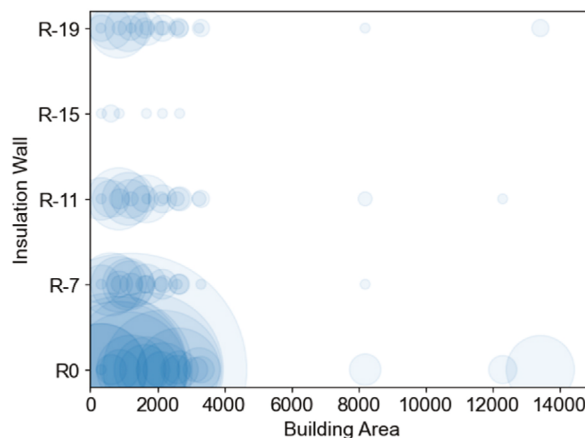
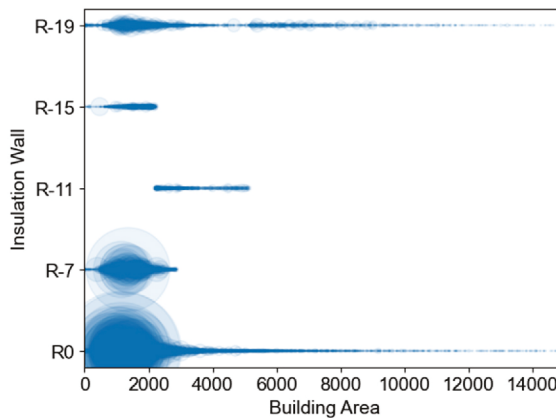


Fig. 7 (c). ResStock building area and insulation distribution.



(d) Enriched building area and insulation distribution

Fig. 7 (d). Enriched building area and insulation distribution.

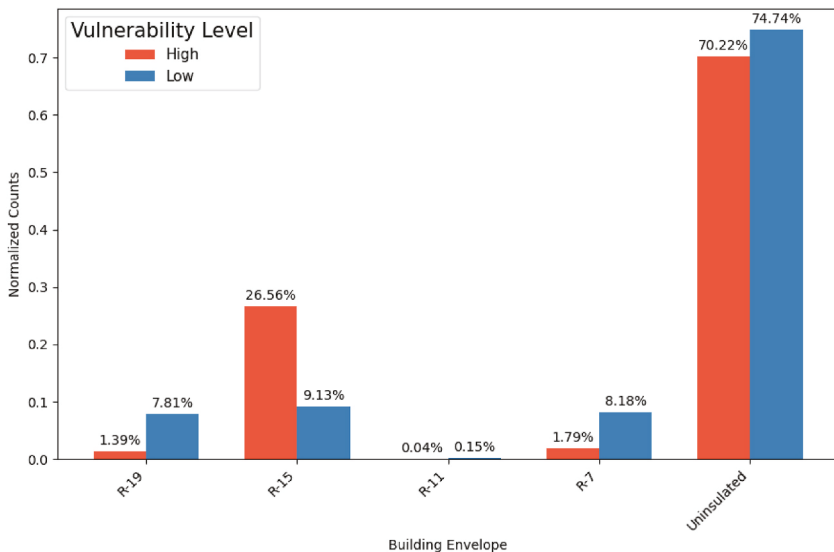


Fig. 8. Building exterior finish based on the year cluster.

Table 5
KS-test summary for the envelope's R value.

Envelope R Value	KS Stat	P value
R-19	0.620	<0
R-15	1.000	0
R-11	0.042	<0
R-7	0.812	<0
Uninsulated	1.00	0

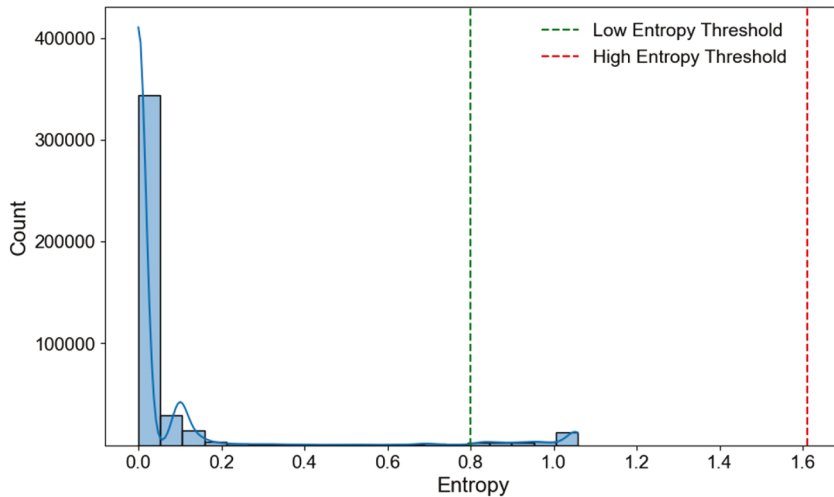
probability are identified as the most probable insulation wall type. Moreover, it is critical to assess potential variability in predicted insulation walls.

Fig. 9 demonstrates the distributions of entropy values for Zillow dataset, where each instance reflects the variability in predicted insulation types. The green and red dashed lines divide instances into three categories: low entropy to the left of the green line, moderate entropy between the green and red lines, and high entropy to the right of the red line. Results show most buildings are identified with low entropy, indicating high confidence and low uncertainty in model predictions, although some probabilistic predictions are found with moderate entropy.

Table 6

Probabilistic prediction of GNBs on insulation walls for nine buildings.

Building Year	Building Area	R-0	R-7	R-11	R-15	R-19	Insulation walls
1960–79	1296.00	0.02	0.98	0.00	0.00	0.00	R-7
2000–09	1641.00	0.00	0.00	0.38	0.16	0.46	R-19
1940–59	2021.00	1.00	0.00	0.00	0.00	0.00	R0
<1940	1633.00	1.00	0.00	0.00	0.00	0.00	R0
1960–79	1320.00	0.02	0.98	0.00	0.00	0.00	R-7
<1940	1216.00	1.00	0.00	0.00	0.00	0.00	R0
1960–79	1000.00	0.02	0.98	0.00	0.00	0.00	R-7
1960–79	2232.00	0.09	0.91	0.00	0.00	0.00	R-7
<1940	896.00	1.00	0.00	0.00	0.00	0.00	R0

**Fig. 9.** Probabilistic entropy analysis for GNB predictions over Zillow data.

3.1.4. Building system

Building systems play a pivotal role in ensuring thermal comfort within buildings, significantly enhancing resilience to heatwaves. A central HVAC system, for example, can maintain comfortable indoor temperature during heatwaves, making buildings more habitable, especially for vulnerable populations such as the elderly or individuals with pre-existing health conditions. This emphasizes the importance of building systems in reducing thermal vulnerability. In this study, the Zillow dataset has been analyzed to categorize building systems, as summarized in **Table 7**. Currently, about 33 % of households use central systems, while 35 % rely on zonal heating systems, and 18 % of homes have at least some form of heating/cooling systems. The disparity in system utilization is evident when comparing high and low-vulnerable groups, as illustrated in **Fig. 10**. The low-vulnerable group predominately uses central heating/cooling systems, which are more effective in maintaining consistent indoor temperature across the entire building. Conversely, the high-vulnerable group is more likely to use zonal heating systems, which typically provide less comprehensive temperature regulation, contributing to thermal discomfort during extreme heatwaves. The higher prevalence of zonal systems among the high-vulnerable population highlights a potential thermal resilience gap, where the absence of centralized systems may exacerbate the impact of heatwaves.

The analysis of heating systems in the Zillow data highlights a significant disparity in the availability of central heating between high and low-vulnerable groups. **Fig. 11 (a)** demonstrate this clear difference with KS statistic of 0.502 and p value < 0.05, indicating a statistically significant contrast. Central heating, which is more effective for whole-building temperature control, appears to be less

Table 7

Heating types and description.

Heating system	Description
Central type	Central, Electric, vent, forced air, forced wall
Heating	Convection, heat pump, hot water, radiant, stream heating
Solar and Wood	Solar, wood-burning
Zone heating	Zone, baseboard, partial, space/suspended
Geo and gravity	Geothermal, oil heating, propane heating, gravity heating
Others	None, other, yes

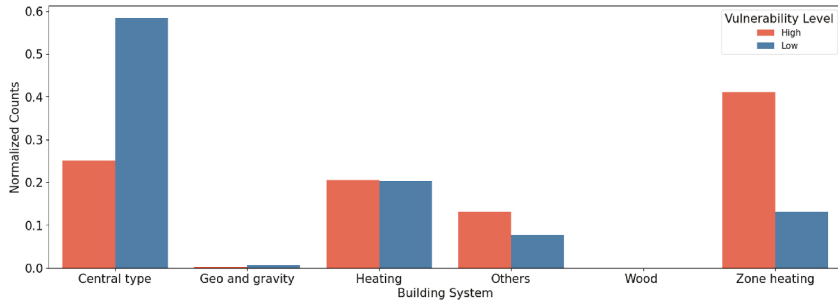


Fig. 10. Normalized counts of building system.

prevalent in high-vulnerability populations. For zonal heating, the distribution shows a similar trend between the groups, but with less pronounced difference. As illustrated in Fig. 11 (b), the KS test statistic of 0.188 and a P value > 0.05 suggest that while both high and low-vulnerable groups use zonal heating There remains a statistically insignificant distinction in the density of usage between the two groups. In summary, both central and zonal heating types are less prevalent in high-vulnerable groups. This suggests that these communities may lack adequate heating and cooling resources in their homes, potentially exacerbating their exposure to thermal stress, especially during extreme weather conditions.

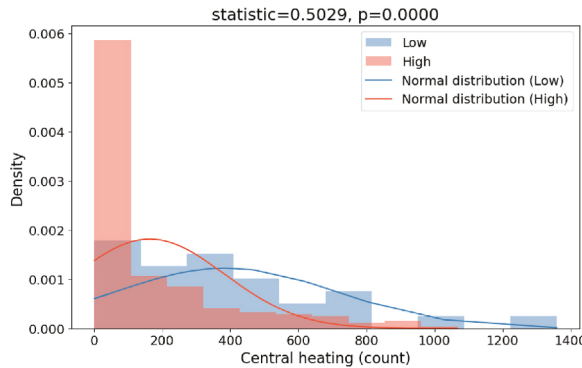
3.1.5. Building surface-to-volume (S/V) ratio

Numerous studies emphasize its importance in understanding and optimizing building thermal characteristics [58,59]. The surface-to-volume (S/V) ratio plays a crucial role in assessing the thermal dynamics of buildings, serving as a key for energy efficiency and performance. Buildings with higher surface-to-volume (S/V) ratios are more susceptible to heat gain or loss due to the increased surface area exposed to the environment, leading to higher energy consumption for heating or cooling. As noted by numerous studies, optimizing the S/V ratio is essential for improving a building's thermal characteristic over resilience. To estimate the S/V ratio, we used the building area data from Zillow, under the assumption of a uniform floor-to-floor height of 10 feet and an approximately square shape [54]. The S/V ratio is calculated using Eq (2):

$$\text{Surface to Volume Ratio} = \left(\text{sqrt} \left(\frac{\text{area}}{\text{stories}} \right) * 4 * 10 + \text{area of floor} \right) / (\text{area} * 10) \quad \text{Eq (2)}$$

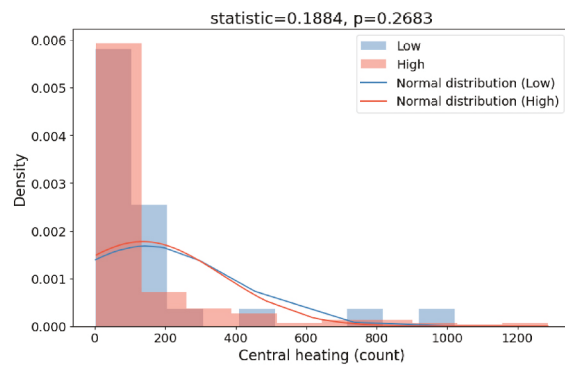
Upon comparing the S/V ratios between high and low-vulnerability groups, as shown in Fig. 12, we observe that the high-vulnerable group generally exhibit higher S/V ratios. The higher ratio indicates increased thermal vulnerability due to greater S/V ratios. This higher ratio indicates increased thermal vulnerability due to greater surface area exposed for heat transfer, resulting in greater energy demands for maintaining comfortable indoor temperatures. A KS test result of 0.25 and a P value of < 0.05 further supports the statistical significance of the differences in S/V ratios between high and low vulnerable groups, highlighting the impact of building form on thermal resilience.

In summary, our analysis demonstrates that buildings associated with low social vulnerability groups typically have fewer stories, fewer rooms, and smaller areas. These building characteristics are critical in influencing thermal mass and inertia, both of which play a pivotal role in moderating the impact of outdoor temperature fluctuations. Lower surface-to-volume ratios in low-vulnerability groups



(a): Probability density of central type between low and high-vulnerable groups

Fig. 11 (a). Probability density of central type between low and high-vulnerable groups.



(b): Probability density of zonal heating between low and high-vulnerable groups

Fig. 11 (b). Probability density of zonal heating between low and high-vulnerable groups.

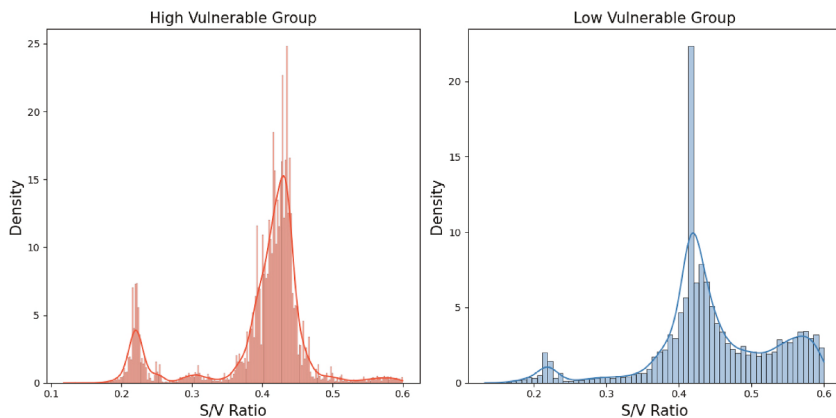


Fig. 12. Distribution of the S/V ratios for the high and low vulnerable group.

also contribute to better thermal performance, as they reduce heat exchange with the environment. On the other hand, high social vulnerability groups, generally residing in buildings with less thermally resilient features, are more exposed to thermal stress. Factors such as higher surface to volume ratios, older building construction, and less advanced heating and cooling systems make these buildings more susceptible to the effects of heatwaves.

4. Discussions

In this study, the KS-2 test was utilized to explore the relationship between building characteristics and the social vulnerability index in Philadelphia. The analysis focused on thermal related building features including building age, area, number of stories, envelope, and systems, comparing high and low vulnerability groups. The findings reveal a correlation, with high thermal vulnerable groups often aligning with higher social vulnerability, and low thermal vulnerable groups with lower social vulnerability. This correlation suggests that integrating thermal features into the SVI could lead to the development of more holistic index that better reflects housing-related risks. Additionally, the pronounced thermal vulnerability among high-vulnerable groups emphasizes the need for targeted strategies to address thermal inequities, particularly in older and inadequately insulated buildings.

4.1. Incorporation of thermal features into the vulnerability index

The integration of thermal features—such as building insulation, air infiltration rates, and other elements of the building envelope—enhances vulnerability indices by providing a more comprehensive view of how buildings contribute to community resilience. These features are key to maintaining indoor thermal comfort and energy efficiency during heatwaves, thereby directly influencing the overall vulnerability of populations. Incorporating such data allows for the creation of more refined strategies aimed at mitigating vulnerability, especially in high-risk areas. For example, communities with high social vulnerability coupled with poorly insulated buildings can be prioritized for retrofitting programs or incentives for energy-efficient upgrades. These targeted interventions not only

enhance the thermal resilience of buildings but also reduce the energy burdens. The interaction between social vulnerability and building thermal performance highlights the need for policies that simultaneously address social and thermal concerns. By exploring these intersections, policymakers can develop adaptation strategies that foster both social and thermal resilience. This approach promotes interdisciplinary collaboration across architecture, engineering, sociology, and public health, encouraging innovating solutions to climate change. Such collaborative efforts are essential to build resilient communities that are better prepared to deal with the intensifying impacts of climate change.

4.2. Thermal equity

The City of Philadelphia has implemented several initiatives to help residents cope with extreme heat, including designated cooling centers, mobile heat health teams, and a residential utility shutoff moratorium during heat emergencies [62]. Additionally, the city offers the Philadelphia Neighborhood Home Preservation Loan Program, which provides loans for retrofitting homes—both for building envelope improvements and system upgrades [63]. However, access to these retrofit loans is contingent on meeting specific credit score requirements, which may inadvertently exclude some residents. Furthermore, the program does not necessarily prioritize older homes, which are often in greater need of such upgrades to improve thermal resilience. The research findings from Philadelphia highlights the importance of informed policymaking to achieve equitable thermal resilience, particularly in communities that are disproportionately affected by extreme heat events. Equitable thermal policies are essential for minimizing disparities in thermal vulnerability. The implementation of energy codes and standards that prioritize heatwave resilience can significantly enhance overall thermal resilience. For instance, provision of single room shelters can ensure fair access to shelter during heatwaves, thus promoting fair access to resources and fostering equitable community resilience. The study's findings, which link building age on thermal vulnerability, highlight the need for targeted retrofit programs. These initiatives can improve the thermal performance of older homes by enhancing their insulation and reducing air infiltration. Prioritizing the retrofits of older homes in high vulnerability areas can help mitigate the thermal stress experienced by disadvantaged populations. By focusing on thermal-centric retrofitting initiatives, communities can better prepare for heatwaves, ensuring that vulnerable populations are less exposed to thermal risks. This approach not only improves building performance but also aligns with broader goals of social equity and resilience, thereby fostering more inclusive and effective outcomes for all.

4.3. Future work

Future research can advance by strategically focusing on the development of high-vulnerable building prototype, emphasizing essential building physics properties to address thermal disparities. This prototype model should encompass critical parameters such as the R-value of the building envelope, insulation quality, infiltration rates, building system, and occupant behaviors during heatwaves. These elements are fundamental to understand how well a building resist heatwave. Focusing on these building physics properties can lead to a deeper understanding of thermal vulnerability. By closely examining R-values and insulation effectiveness, we can identify the most effective retrofitting strategies for improving thermal performance.

5. Conclusion

The increased frequency of extreme heatwaves highlights the urgent need for buildings to adapt to ensure resilience, particularly for vulnerable populations. While these heatwaves disproportionately affect socially vulnerable groups, there has been little focus on how the thermal parameters of buildings in these communities differ. Past research has mainly explored the impact of extreme heatwaves on minority and marginalized groups from a socio-ethnic perspective, often neglecting the role of building thermal performance in resilience. Basic building features are included in current social vulnerability index, but more detailed thermal characteristics are essential to understand how buildings respond to extreme heatwaves. This study bridges that gap by integrating building characteristics from Zillow with thermal data from the ResStock, using a Bayesian GNB. The social vulnerability index from the CDC provides societal vulnerability framework, yet it often overlooks how thermal dynamics impact vulnerability to heatwaves. Our main objective is to assess the resilience of different groups by combining building thermal features and social factors. Key building characteristics such as insulation levels, system types, and building age are analyzed to identify disparities in thermal resilience between high and low vulnerable groups. Statistical method reveals differences in how building attributes like envelope insulation, size, and system types correlate with varying degrees of social vulnerability. The incorporation of thermal features into vulnerability indices provides a significant contribution to understanding social vulnerability in resilience research and emphasizes the importance of considering building thermal features in social-vulnerable index development. A few limitations remain in this study. First, our analysis was confined to the Philadelphia region, and further validation is necessary to ensure the broader applicability of the findings. Second, the data sourced from Zillow may not fully capture the present condition of buildings in the area, introducing potential uncertainty.

This research fills a knowledge gap in between thermal resilience and social vulnerability, exploring how social factors contribute to thermal vulnerability. It lays groundwork for future efforts to develop high vulnerable group's building prototypes that can be used to assess resilience of extreme heatwaves in various geolocation. By focusing on retrofitting older buildings and addressing thermal challenges faced by socioeconomically disadvantaged groups, policymakers can create more targeted interventions. Policymakers can also establish minimum energy standards to ensure thermal reliability during heatwaves. Ensuring fair access to energy, enacting policies to improve thermal resilience, and promote inclusivity in resource planning are central to achieving thermal equity.

CRediT authorship contribution statement

Suman Paneru: Writing – original draft, Software, Methodology, Formal analysis, Data curation, Conceptualization. **Xinyue Xu:** Writing – original draft, Formal analysis, Data curation. **Julian Wang:** Writing – review & editing, Supervision, Project administration, Funding acquisition, Data curation, Conceptualization. **Guangqing Chi:** Writing – review & editing, Supervision, Funding acquisition, Data curation, Conceptualization. **Yuqing Hu:** Writing – review & editing, Validation, Supervision, Project administration, Methodology, Funding acquisition, Data curation, Conceptualization.

Declaration of competing interest

The authors declare that they have no known competing financial interests or personal relationships that could have appeared to influence the work reported in this paper.

Acknowledgment Statement

This research work is supported by the NSF Award # 2215421 CAS-Climate: An Integrated Framework to Investigate Thermal Resilience of Sustainable Buildings and Living Environments for Greater Preparedness to Extreme Temperature Events. Any opinions, findings, and conclusions or recommendations expressed in this material are those of the author(s) and do not necessarily reflect the views of the National Science Foundation. Data provided by Zillow through the Zillow Transaction and Assessment Dataset (ZTRAX). More information on accessing the data can be found at <http://www.zillow.com/ztrax>. The results and opinions are those of the author(s) and do not reflect the position of Zillow Group.

Data availability

Data will be made available on request.

References

- [1] Heat and health [Online], <https://www.who.int/news-room/fact-sheets/detail/climate-change-heat-and-health>. (Accessed 21 June 2024).
- [2] 1.1.5 Heat-Related Mortality. Lancet Countdown 9, 2024, p. 499 [Online]. Available: [www.thelancet.com/pdf/journals/lanpub/PIIS2468-2667\(24\)00055-0.pdf](http://www.thelancet.com/pdf/journals/lanpub/PIIS2468-2667(24)00055-0.pdf). (Accessed 21 June 2024).
- [3] Heatwaves [Online], <https://www.who.int/health-topics/heatwaves>. (Accessed 6 January 2024).
- [4] J. Ballester, et al., Heat-related mortality in Europe during the summer of 2022, Nat. Med. 29 (7) (Jul. 2023) 7, <https://doi.org/10.1038/s41591-023-02419-z>.
- [5] O. Us Epa, Climate change indicators: heat waves [Online]. Available: <https://www.epa.gov/climate-indicators/climate-change-indicators-heat-waves>. (Accessed 6 January 2024).
- [6] D.P. Johnson, A. Stanforth, V. Lulla, G. Luber, Developing an applied extreme heat vulnerability index utilizing socioeconomic and environmental data, Appl. Geogr. 35 (1) (Nov. 2012) 23–31, <https://doi.org/10.1016/j.apgeog.2012.04.006>.
- [7] N. Gouveia, S. Hajat, B. Armstrong, Socioeconomic differentials in the temperature–mortality relationship in São Paulo, Brazil, Int. J. Epidemiol. 32 (3) (Jun. 2003) 390–397, <https://doi.org/10.1093/ije/dyg077>.
- [8] D. Rizmie, L. de Preux, M. Miraldo, R. Atun, Impact of extreme temperatures on emergency hospital admissions by age and socio-economic deprivation in England, Soc. Sci. Med. 308 (Sep. 2022) 115193, <https://doi.org/10.1016/j.socscimed.2022.115193>.
- [9] G. Luber, M. McGeehin, Climate change and extreme heat events, Am. J. Prev. Med. 35 (5) (Nov. 2008) 429–435, <https://doi.org/10.1016/j.amepre.2008.08.021>.
- [10] Z. Xu, G. Fitzgerald, Y. Guo, B. Jalaludin, S. Tong, Impact of heatwave on mortality under different heatwave definitions: a systematic review and meta-analysis, Environ. Int. 89 (90) (Apr. 2016) 193–203, <https://doi.org/10.1016/j.envint.2016.02.007>.
- [11] D.-W. Kim, R.C. Deo, J.-S. Lee, J.-M. Yeom, Mapping heatwave vulnerability in Korea, Nat. Hazards 89 (1) (Oct. 2017) 35–55, <https://doi.org/10.1007/s11069-017-2951-y>.
- [12] CDC/ATSDR social vulnerability index (SVI) [Online]. Available, <https://www.atsdr.cdc.gov/placeandhealth/svi/index.html>. (Accessed 13 September 2023).
- [13] Social vulnerability | national risk index [Online]. Available, <https://hazards.fema.gov/nri/social-vulnerability>. (Accessed 18 March 2023).
- [14] Vulnerability | UNDRR [Online]. Available, <http://www.undrr.org/terminology/vulnerability>. (Accessed 13 September 2023).
- [15] N. Coleman, A. Esmalian, A. Mostafavi, Equitable resilience in infrastructure systems: empirical assessment of disparities in hardship experiences of vulnerable populations during service disruptions, Nat. Hazards Rev. 21 (4) (Nov. 2020) 04020034, [https://doi.org/10.1061/\(ASCE\)NH.1527-6996.0000401](https://doi.org/10.1061/(ASCE)NH.1527-6996.0000401).
- [16] C. Chen, et al., Extreme events, energy security and equality through micro- and macro-levels: concepts, challenges and methods, Energy Res. Social Sci. 85 (Mar. 2022) 102401, <https://doi.org/10.1016/j.erss.2021.102401>.
- [17] K. Thomas, et al., Explaining differential vulnerability to climate change: a social science review, WIREs Clim. Change 10 (2) (2019) e565, <https://doi.org/10.1002/wcc.565>.
- [18] K. Bergstrand, B. Mayer, B. Brumback, Y. Zhang, Assessing the relationship between social vulnerability and community resilience to hazards, Soc. Indicat. Res. 122 (2) (Jun. 2015) 391–409, <https://doi.org/10.1007/s11205-014-0698-3>.
- [19] D. Johnson, Resilience — DOE directives, guidance, and delegations [Online]. Available: https://www.directives.doe.gov/terms_definitions/resilience. (Accessed 13 August 2023).
- [20] fema_planning-resilient-communities_fact-sheet.pdf [Online]. Available, https://www.fema.gov/sites/default/files/documents/fema_planning-resilient-communities_fact-sheet.pdf. (Accessed 13 September 2023).
- [21] Resilience | UNDRR [Online]. Available, <http://www.undrr.org/terminology/resilience>. (Accessed 13 September 2023).
- [22] Resilience roadmap [Online]. Available, <https://www.nrel.gov/resilience-planning-roadmap/>. (Accessed 13 September 2023).
- [23] Risk and resilience - oecd [Online]. Available, <https://www.oecd.org/dac/conflict-fragility-resilience/risk-resilience/>. (Accessed 13 September 2023).
- [24] Resilience [Online]. Available, <https://www.apa.org/topics/resilience>. (Accessed 13 September 2023).
- [25] National resilience guidance | FEMA.gov [Online]. Available, <https://www.fema.gov/emergency-managers/national-preparedness/plan/resilience-guidance>. (Accessed 16 September 2023).
- [26] E. Cox, I hope they shouldn't happen': social vulnerability and resilience to urban energy disruptions in a digital society in Scotland, Energy Res. Social Sci. 95 (Jan. 2023) 102901, <https://doi.org/10.1016/j.erss.2022.102901>.

[27] L. Nicholls, Y. Strengers, Heatwaves, cooling and young children at home: integrating energy and health objectives, *Energy Res. Social Sci.* 39 (May 2018) 1–9, <https://doi.org/10.1016/j.erss.2017.10.002>.

[28] M. Salimi, S.G. Al-Ghamdi, Climate change impacts on critical urban infrastructure and urban resiliency strategies for the Middle East, *Sustain. Cities Soc.* 54 (Mar. 2020) 101948, <https://doi.org/10.1016/j.scs.2019.101948>.

[29] B.-J. He, J. Wang, J. Zhu, J. Qi, Beating the urban heat: situation, background, impacts and the way forward in China, *Renew. Sustain. Energy Rev.* 161 (Jun. 2022) 112350, <https://doi.org/10.1016/j.rser.2022.112350>.

[30] M. Ulrichs, R. Slater, C. Costella, Building resilience to climate risks through social protection: from individualised models to systemic transformation, *Disasters* 43 (S3) (2019) S368–S387, <https://doi.org/10.1111/disa.12339>.

[31] O. US EPA, Heat islands and equity [Online], <https://www.epa.gov/heatislands/heat-islands-and-equity>. (Accessed 11 October 2024).

[32] B.M. Jesdale, R. Morello-Frosch, L. Cushing, The racial/ethnic distribution of heat risk-related land cover in relation to residential segregation, *Environ. Health Perspect.* 121 (7) (Jul. 2013) 811–817, <https://doi.org/10.1289/ehp.1205919>.

[33] M. Guardaro, D.M. Hondula, J. Ortiz, C.L. Redman, Adaptive capacity to extreme urban heat: the dynamics of differing narratives, *Clim. Risk Manag.* 35 (Jan. 2022) 100415, <https://doi.org/10.1016/j.crm.2022.100415>.

[34] M. Guardaro, M. Messerschmidt, D.M. Hondula, N.B. Grimm, C.L. Redman, Building community heat action plans story by story: a three neighborhood case study, *Cities* 107 (2020), <https://doi.org/10.1016/j.cities.2020.102886>.

[35] S.N.A. Codjoe, et al., Impact of extreme weather conditions on healthcare provision in urban Ghana, *Soc. Sci. Med.* 258 (2020), <https://doi.org/10.1016/j.socscimed.2020.113072>.

[36] Z. Hamstead, et al., Thermally resilient communities: creating a socio-technical collaborative response to extreme temperatures, *Build. Cities* 1 (1) (2020) 218–232, <https://doi.org/10.5334/bc.15>.

[37] H. Omrany, A. Ghaffarianhoseini, A. Ghaffarianhoseini, K. Raahemifar, J. Tookey, Application of passive wall systems for improving the energy efficiency in buildings: a comprehensive review, *Renew. Sustain. Energy Rev.* 62 (Sep. 2016) 1252–1269, <https://doi.org/10.1016/j.rser.2016.04.010>.

[38] L. Toledo, P.C. Cropper, A.J. Wright, *Vulnerability and resilience in energy efficient homes: thermal response to heatwaves*, in: *Presented at the Proceedings of 33rd PLEA International Conference: Design to Thrive, vol. 2017, PLEA, 2017*, pp. 875–882.

[39] G. Hatvani-Kovacs, M. Belusko, N. Skinner, J. Pockett, J. Boland, Drivers and barriers to heat stress resilience, *Sci. Total Environ.* 571 (2016) 603–614, <https://doi.org/10.1016/j.scitotenv.2016.07.028>.

[40] I. Ahmed, M. van Esch, F. van der Hoeven, Heatwave vulnerability across different spatial scales: insights from the Dutch built environment, *Urban Clim.* 51 (2023), <https://doi.org/10.1016/j.uclim.2023.101614>.

[41] M. Gangolells, M. Casals, Resilience to increasing temperatures: residential building stock adaptation through codes and standards, *Build. Res. Inf.* 40 (6) (2012) 645–664, <https://doi.org/10.1080/09613218.2012.698069>.

[42] S. Flores-Larsen, C. Filippín, F. Bre, New metrics for thermal resilience of passive buildings during heat events, *Build. Environ.* 230 (Feb. 2023) 109990, <https://doi.org/10.1016/j.buildenv.2023.109990>.

[43] S. Flores-Larsen, C. Filippín, Energy efficiency, thermal resilience, and health during extreme heat events in low-income housing in Argentina, *Energy Build.* 231 (Jan. 2021) 110576, <https://doi.org/10.1016/j.enbuild.2020.110576>.

[44] J. Bambara, A.K. Athienitis, U. Eicker, Residential densification for positive energy districts, *Front. Sustain. Cities* 3 (2021), <https://doi.org/10.3389/frsc.2021.630973>.

[45] J. Górski, A.P. Nowak, M. Kołataj, Resilience of raw-earth technology in the climate of middle europe based on analysis of experimental building in pasłek in Poland, *Sustain. Switz.* 13 (23) (2021), <https://doi.org/10.3390/su132313246>.

[46] R. Caro, J.J. Sendra, Evaluation of indoor environment and energy performance of dwellings in heritage buildings. The case of hot summers in historic cities in Mediterranean Europe, *Sustain. Cities Soc.* 52 (2020), <https://doi.org/10.1016/j.scs.2019.101798>.

[47] A.-L. Balogun, et al., Assessing the potentials of digitalization as a tool for climate change adaptation and sustainable development in urban centres, *Sustain. Cities Soc.* 53 (Feb. 2020) 101888, <https://doi.org/10.1016/j.scs.2019.101888>.

[48] M. Kaufmann, S. Veenman, S. Haarbosch, E. Jansen, How policy instruments reproduce energy vulnerability - a qualitative study of Dutch household energy efficiency measures, *Energy Res. Social Sci.* 103 (Sep. 2023) 103206, <https://doi.org/10.1016/j.erss.2023.103206>.

[49] K. Müller, Objective' numbers in energy research: trust, order, governing and methodology, *Energy Res. Social Sci.* 106 (Dec. 2023) 103310, <https://doi.org/10.1016/j.erss.2023.103310>.

[50] New approaches to assessing vulnerability and resilience [Online], <https://search.informit.org/doi/epdf/10.3316/ielapa.369155833780624>. (Accessed 26 October 2023).

[51] Zillow: real estate, apartments, mortgages & home values [Online], <https://www.zillow.com/>. (Accessed 20 November 2023).

[52] ResStock analysis tool [Online], <https://www.nrel.gov/buildings/restock.html>. (Accessed 23 January 2024).

[53] M. Aksozen, M. Daniel, U. Hessler, N. Kohler, Building age as an indicator for energy consumption, *Energy Build.* 87 (Jan. 2015) 74–86, <https://doi.org/10.1016/j.enbuild.2014.10.074>.

[54] Y. Feng, Q. Duan, X. Chen, S.S. Yakkali, J. Wang, Space cooling energy usage prediction based on utility data for residential buildings using machine learning methods, *Appl. Energy* 291 (Jun. 2021) 116814, <https://doi.org/10.1016/j.apenergy.2021.116814>.

[55] S. Mirrahimi, M.F. Mohamed, L.C. Haw, N.L.N. Ibrahim, W.F.M. Yusoff, A. Aflaki, The effect of building envelope on the thermal comfort and energy saving for high-rise buildings in hot-humid climate, *Renew. Sustain. Energy Rev.* 53 (Jan. 2016) 1508–1519, <https://doi.org/10.1016/j.rser.2015.09.055>.

[56] H. Johra, P. Heiselberg, J.L. Dréau, Influence of envelope, structural thermal mass and indoor content on the building heating energy flexibility, *Energy Build.* 183 (Jan. 2019) 325–339, <https://doi.org/10.1016/j.enbuild.2018.11.012>.

[57] A. Afram, F. Janabi-Sharifi, Review of modeling methods for HVAC systems, *Appl. Therm. Eng.* 67 (1) (Jun. 2014) 507–519, <https://doi.org/10.1016/j.aplthermaleng.2014.03.055>.

[58] M.T. Araji, Surface-to-volume ratio: how building geometry impacts solar energy production and heat gain through envelopes, *IOP Conf. Ser. Earth Environ. Sci.* 323 (1) (Aug. 2019) 012034, <https://doi.org/10.1088/1755-1315/323/1/012034>.

[59] B. D'Amico, F. Pomponi, A compactness measure of sustainable building forms, *R. Soc. Open Sci.* 6 (6) (Jun. 2019) 181265, <https://doi.org/10.1098/rsos.181265>.

[60] E. Wilson, et al., End-Use Load Profiles for the U.S. Building Stock: Methodology and Results of Model Calibration, Validation, and Uncertainty Quantification, Mar. 2022, <https://doi.org/10.2172/1854582>. NREL/TP-5500-80889, 1854582, MainId:78667.

[61] C. E. Shannon, "A Mathematical Theory of Communication".

[62] Heat health emergency | Services, City of Philadelphia, <https://www.phila.gov/services/safety-emergency-preparedness/extreme-weather/heat-health-emergency/>. (Accessed 11 October 2024).

[63] Final-flyer3_27_19-clarifi.pdf [Online], https://www.phila.gov/media/20190416105735/Final-flyer3_27_19-clarifi.pdf. (Accessed 11 October 2024).